LA-UR- 08-4368

Approved for public release;
distribution is unlimited.

Title:	LEAST-SQUARES FINITE ELEMENT METHODS FOR QUANTUM CHROMODYNAMICS
Author(s):	J. BRANNICK C. KETELSEN T. MANTEUFFEL S. MCCORMICK
Intended for:	JOURNAL: SIAM JOURNAL ON SCIENTIFIC COMPUTING

Los Alamos
NATIONAL LABORATORY
EST.1943

Form 836 (7/06)

1 2

LEAST-SQUARES FINITE ELEMENT METHODS FOR QUANTUM CHROMODYNAMICS

J. BRANNICK[1], C. KETELSEN[2], T. MANTEUFFEL[2], S. MCCORMICK[2]

Abstract. A significant amount of the computational time in large Monte Carlo simulations of lattice quantum chromodynamics (QCD) is spent inverting the discrete Dirac operator. Unfortunately, traditional covariant finite difference discretizations of the Dirac operator present serious challenges for standard iterative methods. For interesting physical parameters the discretized operator is large and ill-conditioned, and has random coefficients. More recently, adaptive algebraic multigrid (AMG) methods have been shown to be effective preconditioners for Wilson's discretization [1] [2] of the Dirac equation. This paper presents an alternate discretization of the Dirac operator based on least-squares finite elements. The discretization is systematically developed and physical properties of the resulting matrix system are discussed. Finally, numerical experiments are presented that demonstrate the effectiveness of adaptive smoothed aggregation (αSA) multigrid as a preconditioner for the discrete field equations resulting from applying the proposed least-squares FE formulation to a simplified test problem, the 2d Schwinger model of quantum electrodynamics (QED).

Key words. quantum chromodynamics, lattice, finite element, multigrid, smoothed aggregation

AMS subject classifications. 81V05, 65N30, 65N55

1. Introduction. Quantum Chromodynamics (QCD) is the leading theory in the Standard Model of particle physics of the strong interactions between color charged particles (quarks) and the particles that bind them (gluons). Analogous to the way that electrically charged particles exchange photons to create an electromagnetic field, quarks exchange gluons to form a very strong color force field. Contrary to the electromagnetic force, the strong force binding quarks does not get weaker as the particles get farther apart. As such, at long distances (low energies) quarks have not been observed independently in experiment and due to their strong coupling, perturbative techniques, that have been so successful in describing weak interactions in Quantum Electrodynamics (QED), diverge for the low-energy regime of QCD. Instead, hybrid Monte Carlo (HMC) simulations are employed in an attempt to numerically predict physical observables in accelerator experiments [6].

A main computational bottleneck in an HMC simulation is computation of the so-called *fermion propagator*; another name for the inverse of the discrete Dirac operator. This process accounts for a large amount of the overall simulation time. For realistic physical parameter values, the Dirac operator has random coefficients and is extremely ill-conditioned. The two main parameters of interest are the temperature (β) of the background gauge field and the quark mass (m). For small temperature values ($\beta < 5$), the entries in the Dirac matrix become extremely disordered. Moreover, as the quark mass approaches its true physical value, the performance of the community standard Krylov solvers degrades; a phenomenon known as *critical slowing down*. As a result, the development of sophisticated preconditioners for computing propagators has been a priority in the QCD community for some time. Recently, multilevel preconditioners like algebraic multigrid (AMG) have proved to be especially effective at speeding up simulation time [1] [2].

[1]Department of Mathematics, Pennsylvania State University, Email: brannick@psu.ed

[2]Department of Applied Mathematics, University of Colorado at Boulder, Email: ketelsen@colorado.edu, tmanteuf@colorado.edu, stevem@colorado.edu

While these works have focused mainly on the task of developing better iterative methods for traditional discretizations of the continuous Dirac operator, it is also important to investigate alternate discretizations as a way to decrease the computational cost of QCD simulations.

In the remainder of §1, we introduce the continuum Dirac equation for the full QCD model. We then describe the simplified 2D Schwinger model of QED, which will be the focus of the rest of this paper. In §2, we discuss the challenges presented by the discrete Dirac equation. We discuss traditional finite difference discretizations of the field equations, and their undesirable properties. The least-squares discretization of the Dirac equations is developed and several important properties of the resulting system are discussed, including gauge covariance of the propagator, chiral symmetry, and the problem of species doubling. In §3, we describe the use of an adaptive algebraic multilevel method as a preconditioner for the solution process. Finally, in §4, we make some concluding remarks.

1.1. The Continuous Dirac Operator. The Dirac equation is the relativistic analogue of the Schrodinger equation. Depending on the specific gauge theory the operator can take on several forms, the most general form of which is given by

$$\mathcal{D}\psi = \sum_{\mu=1}^{d} \gamma^{\mu} \otimes (\partial_{\mu} - i\mathcal{A}_{\mu})\,\psi + m\psi. \tag{1.1}$$

Here, d is the problem dimension, the γ^{μ}'s are matrix coefficients, ∂_{μ} is the usual partial derivative in the x_{μ} direction, m is the particle mass, and $\mathcal{A}_{\mu}(x)$ is the gauge field representing the force carriers. Operator $\mathcal{D}$ acts on $\psi : \mathbb{R}^d \mapsto \mathbb{C}^4 \otimes \mathbb{C}^3$, a tensor field (multicomponent wavefunction) describing the particle. These symbols take on different values and dimensions depending on the gauge theory. In full QCD, $d = 4$ (three spatial and one time dimension), γ^{μ} are the 4×4 anticommuting complex Dirac matrices, $\mathcal{A}_{\mu}(x) \in \mathrm{su}(3)$ are 3×3, traceless, Hermitian matrices that describe the gluon fields. We mention in passing that the unknown function, ψ, is a 12-component wavefunction with each component corresponding to a quark with a specific color (red, green, or blue), spin (up or down), and energy (positive or negative).

The Dirac equation does not necessarily have to describe the behavior of quarks, specifically. In general, it can describe the behavior of any fermion, including electrons. Because of the considerable complexity of the full QCD model, it is common practice to consider the simplified 2D Schwinger model of QED [1], which models the interaction between electrons and photons, when developing algorithms for QCD. In this case, only two spatial directions are considered, the particle wavefunction, ψ, has only two components (spin-up and spin-down), and the photon field, $\mathcal{A}_{\mu}(x)$, is a real-valued scalar. Though an extreme simplification, the discrete Dirac operator associated with the Schwinger model presents many of the same numerical difficulties found in the full physical model.

1.2. Model Problem. Let the domain be $\Gamma = [0,1] \times [0,1]$, and let $\mathcal{V}_c$ be the complex-valued periodic functions in $H^1(\Gamma)$. We introduce the shorthand notation $\nabla_{\mu} = (\partial_{\mu} - i\mathcal{A}_{\mu})$ for the μ^{th} covariant derivative. The continuum Dirac equation for the 2D Schwinger model with periodic boundary conditions is given by

$$\begin{aligned} \mathcal{D}(\mathcal{A})\psi = [\gamma_1\nabla_x + \gamma_2\nabla_y + mI]\psi = f \quad \text{in } \Gamma, \\ \psi(0,y) = \psi(1,y), \\ \psi(x,0) = \psi(x,1), \end{aligned} \tag{1.2}$$

where $\mathcal{A}(x,y) = [\mathcal{A}_1(x,y), \mathcal{A}_2(x,y)]^t$ is the periodic gauge field, and $\psi(x,y) = [\psi_u(x,y), \psi_d(x,y)]^t \in \mathcal{V}_c^2$ is the fermion field with ψ_u and ψ_d representing the spin-up and spin-down particles, respectively. In 2D, the γ-matrices correspond to the Pauli spin matrices of quantum mechanics. They are

$$\gamma_1 = \begin{bmatrix} 0 & 1 \\ 1 & 0 \end{bmatrix}, \quad \gamma_2 = \begin{bmatrix} 0 & -i \\ i & 0 \end{bmatrix}.$$

Note that (1.2) appears in matrix notation as

$$\begin{bmatrix} m & \nabla_x - i\nabla_y \\ \nabla_x + i\nabla_y & m \end{bmatrix} \begin{bmatrix} \psi_u \\ \psi_d \end{bmatrix} = \begin{bmatrix} f_u \\ f_d \end{bmatrix} \tag{1.3}$$

A word on notation. In this paper we use three different types of objects: continuum functions, finite element functions, and discrete vectors. Continuum functions are represented by scripted and Greek symbols, as in $\mathcal{A}$, f, and ψ. Finite element functions are represented by the similar symbols, but with a superscript h, as in A^h, f^h, and ψ^h. Finally, discrete vectors appear with an underbar, as in $\underline{A}$, $\underline{f}$, and $\underline{\psi}$. Operators in the continuum are denoted by scripted symbols, as in $\mathcal{D}$, while discrete operators will be represented by bold symbols, as in $\mathbb{D}$. In any case, the nature of the operator should always be clear from the context.

2. The Discrete Dirac Operator. One computationally intensive part of a QCD simulation is the repeated solution of linear systems of the form

$$\mathbb{D}(\underline{A})\,\underline{\psi} = \underline{f},$$

where $\mathbb{D}$ is the matrix Dirac operator. Solution of systems of this type are needed both for computing observables and for generating gauge fields with the correct probabilistic characteristics [2]. In these processes, $\mathbb{D}$ must be inverted numerous times with many different right hand sides and gauge configurations. Because the background fields must be varied, the entries in the matrix themselves change throughout a simulation.

In the discrete setting, Γ is replaced by an $n \times n$ periodic lattice. Let $\mathcal{N}_c$ be the space of discrete complex valued vectors with values associated with the sites on the lattice. Then, the continuum wavefunction ψ becomes $\underline{\psi} = [\underline{\psi}_u, \underline{\psi}_d]^t \in \mathcal{N}_c^2$, which specifies complex values of both the spin-up and spin-down components of the fermion field at each lattice site. Similarly, the source term, f, becomes $\underline{f} = [\underline{f}_u, \underline{f}_d]^t \in \mathcal{N}_c^2$. Let $\mathcal{E}$ be the space of discrete real valued vectors with values associated with the lattice links. The continuum gauge field $\mathcal{A}$ becomes $\underline{A} = [\underline{A}_1, \underline{A}_2]^t \in \mathcal{E}$, where $\underline{A}_1$ specifies the values of the gauge field on the horizontal lattice links, and $\underline{A}_2$ specifies the values of the gauge field on the vertical lattice links.

Traditional discretization methods for the Dirac operator are based on covariant finite differences (CoFD) [9]. Formulations of this type are problematic from a

computational perspective because they frequently introduce numerical instabilities into the solution process, which are sometimes remedied by adding artificial stabilization terms. Furthermore, the resulting discrete operator is not usually Hermitian and positive definite. It is standard practice to solve the discrete form of the normal equations,

$$\mathbb{D}^*\mathbb{D}\underline{\psi} = \mathbb{D}^*\underline{f} \tag{2.1}$$

rather than treating the original system directly. This decreases the efficiency of the simulation since $\mathbb{D}^*\mathbb{D}$ has a larger stencil than $\mathbb{D}$ and a potentially larger condition number. The proposed discretization, based on least-squares finite elements, produces a discrete operator that is hermitian positive definite (HPD) and has a smaller stencil what than the CoFD method produces.

2.1. The Least-Squares Discretization. We formulate the solution to (1.2) in terms of a minimization principle:

$$\psi^* = \arg\min_{\psi \in \mathcal{V}_c^2} \|\mathcal{D}\psi - f\|_0^2, \tag{2.2}$$

where $\mathcal{V}_c$ is the space of continuous, periodic, complex-valued, H^1 functions defined previously. Eq.(2.2) is equivalent to the weak form

$$\text{Find } \psi \in \mathcal{V}_c^2 \text{ s.t. } \langle \mathcal{D}\psi, \mathcal{D}v\rangle = \langle f, \mathcal{D}v\rangle \qquad \forall v \in \mathcal{V}_c^2, \tag{2.3}$$

where $\langle \cdot, \cdot \rangle$ is the usual L^2 inner product. If ψ is sufficiently smooth, (2.3) is formally equivalent to

$$\text{Find } \psi \in \mathcal{V}_c^2 \text{ s.t. } \langle \mathcal{D}^*\mathcal{D}\psi, v\rangle = \langle \mathcal{D}^* f, v\rangle \qquad \forall v \in \mathcal{V}_c^2.$$

Thus, we can think of the least-squares formulation of the problem as being loosely equivalent to solving the continuum normal equations, $\mathcal{D}^*\mathcal{D}\psi = \mathcal{D}^* f$, by the Galerkin method. Looking at the *formal normal* operator, $\mathcal{D}^*\mathcal{D}$, can often give insight into the potential success of the least-squares formulation:

$$\mathcal{D}^*\mathcal{D} = \begin{bmatrix} m & -\nabla_x + i\nabla_y \\ -\nabla_x - i\nabla_y & m \end{bmatrix} \begin{bmatrix} m & \nabla_x - i\nabla_y \\ \nabla_x + i\nabla_y & m \end{bmatrix}$$

$$= \begin{bmatrix} m^2 - \nabla_x^2 - \nabla_y^2 & 0 \\ 0 & m^2 - \nabla_x^2 - \nabla_y^2 \end{bmatrix}.$$

In the Schwinger case, the formal normal has uncoupled Laplacian-like operators on the main diagonal. Though these are not simple constant coefficient Laplacians (because they include the random background fields), their Hermitian positive definite scalar character should lend themselves to a more efficient treatment by multigrid methods.

The least-squares solution is obtained by requiring that the minimization problem posed in (2.2), and thus, the weak form given in Eq.(2.3), hold for all functions in a finite-dimensional space $\mathcal{V}_c^h \subset \mathcal{V}_c$. That is, our solution must satisfy

$$\text{Find } \psi^h \in \left(\mathcal{V}_c^h\right)^2 \text{ s.t. } \left\langle \mathcal{D}\psi^h, \mathcal{D}v^h \right\rangle = \left\langle f^h, \mathcal{D}v^h \right\rangle \quad \forall v^h \in \left(\mathcal{V}_c^h\right)^2. \tag{2.4}$$

In analogy to the nodal setting, each elementary square on the lattice, or *plaquette*, is represented by a quadrilateral finite element. We equate any $\underline{f} \in \mathcal{N}_c^2$ with the bilinear function $f^h \in \left(\mathcal{V}_c^h\right)^2$, where $\mathcal{V}_c^h = \text{span}\{\phi_j\}_{j=1}^{n^2}$ is taken to be the space of periodic bilinear finite element functions over the complex numbers. Here, ϕ_j is the usual bilinear nodal basis function associated with lattice site x_j. Similarly, we equate any $\underline{A} \in \mathcal{E}$ with $A^h \in \mathcal{W}^h$, where $\mathcal{W}^h$ is the Nedelec space over the real numbers. In this context, the x-component of the gauge field, A_1^h, is represented by a linear combination of edge functions, associated with the horizontal lattice links. The corresponding basis functions are constant along the link, and have support only in the elements above and below. They take on the constant value 1.0 on the link, and are linear in y, decaying to 0.0 at the opposite horizontal links in their shared elements (see Figure 2.1a). The basis for the y-component, A_2^h, is similar, but oriented on the vertical links (see Figure 2.1b) [8].

The maps between members of the discrete spaces $\mathcal{N}_c$ and $\mathcal{E}$, and the finite element spaces $\mathcal{V}_c^h$ and $\mathcal{W}^h$, are quite trivial. To see this, let

$$\underline{f} = \begin{bmatrix} f_1 \\ \vdots \\ f_j \\ \vdots \\ f_{n^2} \end{bmatrix} \quad \text{and} \quad f^h = \sum_{j=1}^{n^2} b_j \phi_j.$$

Note that f_j is the value of the discrete field at the jth lattice site, and the finite element field, f^h, takes on the value b_j at the jth lattice site. In order for the two field descriptions to be consistent, we must have $f_j = b_j, \ j = 1, \ldots, n^2$. Thus, the mapping between $\mathcal{N}_c$ and $\mathcal{V}_c^h$ is simply the bijective identity map between the entries of the nodal vector and the coefficients of the finite element function. A similar analysis shows that the same relationship holds between the gauge field edge values of $\underline{A} \in \mathcal{E}$ and the coefficients of the Nedelec representation of the gauge field $A^h \in \mathcal{W}^h$.

We wish to use the least-squares formalism described above to approximate the solution of (2.1). This process should accept source data, $\underline{f}$, defined on the nodes, and gauge field data, $\underline{A}$, prescribed on the lattice links, and return the discrete wavefunction $\underline{\psi}$, defined at the nodes. We do this by mapping $\underline{f}$ and $\underline{A}$ into their respective finite element spaces , solving the weak formulation (2.4), and mapping the resulting finite element solution back to $\mathcal{N}_c^2$. This process is summarized in Algorithm 1:

ALGORITHM 1: Least-Squares Dirac Solve

- *Input:* Gauge field $\underline{A}$, source term $\underline{f}$.
- *Output:* Wavefunction $\underline{\psi}$.

1. Map $\underline{A} \mapsto A^h \in \mathcal{W}^h$.
2. Map $\underline{f} \mapsto f^h \in \left(\mathcal{V}_c^h\right)^2$.
3. Find $\psi^h \in \left(\mathcal{V}_c^h\right)^2$ s.t. $\left\langle \mathcal{D}\psi^h, \mathcal{D}v^h \right\rangle = \left\langle f^h, \mathcal{D}v^h \right\rangle \quad \forall v^h \in \left(\mathcal{V}_c^h\right)^2$, where $\mathcal{A} = A^h$.
4. Map $\psi^h \mapsto \underline{\psi} \in \mathcal{N}_c^2$.

It is not immediately obvious how to implement the solution of the weak form (2.4), which appears in Step 3 of Algorithm 1. Using the nodal basis for $\mathcal{V}_c^h$, we can establish the following matrix equation for this process:

$$\mathbb{A}u = \mathbb{G}b,$$

where the entries in vectors u and b are the coefficients in the expansions of ψ^h and f^h, respectively, and the elements of the matrices are given by

$$\left[\mathbb{A}\right]_{j,k} = \left\langle \mathcal{D}\phi_k, \mathcal{D}\phi_j \right\rangle, \tag{2.5}$$

$$\left[\mathbb{G}\right]_{j,k} = \left\langle \phi_k, \mathcal{D}\phi_j \right\rangle. \tag{2.6}$$

Then, Step 3 in Algorithm 1 can be replaced by computing

$$u = \mathbb{A}^{-1}\mathbb{G}b.$$

and setting

$$\psi^h = \sum_{j=1}^{n^2} u_j \phi_j.$$

Recalling the relationship between the entries of $\underline{\psi}$ and $\underline{f}$, and the coefficients in the expansion of ψ^h and f^h, we see that Steps 2-4 in Algorithm 1 can be replaced by

$$\underline{\psi} = \mathbb{A}^{-1}\mathbb{G}\underline{f}. \tag{2.7}$$

It is easy to see that, for $m > 0$, both $\mathbb{A}$ and $\mathbb{G}$ are nonsingular. For $\mathbb{A}$, note that by construction $\mathbb{A}$ is Hermitian positive semi-definite and if it were singular, then the original Dirac operator would be singular on some element of $\left(\mathcal{V}_c^h\right)^2$. Also, note that, from the form of the formal normal, it is clear that $\mathbb{A}$ is block-diagonal. That is,

$$\mathbb{A} = \begin{bmatrix} \mathbb{A}_u & 0 \\ 0 & \mathbb{A}_d \end{bmatrix}. \tag{2.8}$$

To see that $\mathbb{G}$ is nonsingular we look more closely at the block form of $\mathbb{G}$. Recall the matrix form of the continuous Dirac operator given in (1.3). Then,

$$\mathbb{G} = \begin{bmatrix} m\mathbb{M} & \mathbb{B}_x - i\mathbb{B}_y \\ \mathbb{B}_x + i\mathbb{B}_y & m\mathbb{M} \end{bmatrix}, \tag{2.9}$$

where

$$\begin{aligned} [\mathbb{M}]_{j,k} &= \langle \phi_k, \phi_j \rangle, \\ [\mathbb{B}_x]_{j,k} &= \langle \phi_k, \nabla_x \phi_j \rangle, \\ [\mathbb{B}_y]_{j,k} &= \langle \phi_k, \nabla_y \phi_j \rangle. \end{aligned}$$

Notice that $\mathbb{G}$ is a skew-Hermitian matrix shifted by mI. Thus, all eigenvalues of $\mathbb{G}$ are of the form $m + is$ for some $s \in \mathbb{R}$.

2.2. Gauge Covariance of the Quark Propagator. A desirable property of any QCD (or QED) theory is that the fermion propagator must transform covariantly under local gauge transformations. These local transformations can be thought of as redefining the coordinate system of the background gauge field at different points in space. In full QCD, for instance, applying a gauge transformation to wavefunction ψ at position x changes the color reference frame at that particular point. A trivial example would be if the roles of blue and red particles where switched at one or several points in the domain.

Suppose we have a fermion field, ψ, defined in a color reference frame, $\mathcal{C}$. Now suppose we are given a gauge transformation, $\Omega(x) \in \mathrm{SU}(3)$, that transforms the field into a new reference frame, $\widetilde{\mathcal{C}}$, according to $\psi \mapsto \Omega(x)\psi$. Note that elements of SU(3) are 3×3 unitary matrices with determinant 1. Propagator $\mathcal{D}^{-1}$ transforms covariantly if, given $\Omega(x)$, it is possible to specify a modified propagator, $\widetilde{\mathcal{D}}^{-1}$, such that applying $\widetilde{\mathcal{D}}^{-1}$ to a field in $\widetilde{\mathcal{C}}$ is equivalent to applying the original propagator to the field in $\mathcal{C}$ and then transforming the result to $\widetilde{\mathcal{C}}$. In other words, given $\Omega(x)$, we must be able to specify $\widetilde{\mathcal{D}}^{-1}$ such that

$$\widetilde{D}^{-1}\Omega(x)\psi = \Omega(x)D^{-1}\psi.$$

It should not be surprising that the correct transformation of $\mathcal{D}^{-1}$ requires modifying the background gauge fields that the Dirac operator is built upon. It is helpful to look at an example of this concept in the 2D Schwinger model of QED, where the gauge transformation comes from U(1). That is, the gauge transformation, $\Omega(x, y)$, is a complex scalar with unit magnitude.

EXAMPLE 1. Consider the continuum 2D Schwinger model. From (1.1) the Dirac operator is

$$\mathcal{D} = [\gamma_1 \nabla_x + \gamma_2 \nabla_y + mI] = \begin{bmatrix} m & \nabla_x - i\nabla_y \\ \nabla_x + i\nabla_y & m \end{bmatrix}, \tag{2.10}$$

where ∇_x and ∇_y are the covariant derivative in the x, and y directions, respectively. We want to show that, given a U(1) transformation, $\Omega(x) = e^{i\theta(x,y)}$, we can modify the covariant derivative operators, ∇_x, ∇_y, so that the propagator, $\mathcal{D}^{-1}$, transforms

covariantly. Here, θ is a real-valued periodic continuous function in H^1. We denote the space of such functions by $\mathcal{V}_{\tilde{h}} \subset \mathcal{V}_{\tilde{c}}$. To see this, set

$$e^{i\theta}\left[\gamma_1\nabla_x + \gamma_2\nabla_y + mI\right]^{-1}\psi = \xi$$

implying

$$\begin{aligned}
\psi &= \left[\gamma_1\nabla_x + \gamma_2\nabla_y + mI\right]e^{-i\theta}\xi, \\
\psi &= \gamma_1\nabla_x\left(e^{-i\theta}\xi\right) + \gamma_2\nabla_y\left(e^{-i\theta}\xi\right) + me^{-i\theta}\xi, \\
\psi &= \gamma_1\left(\partial_x - i\mathcal{A}_1\right)\left(e^{-i\theta}\xi\right) + \gamma_2\left(\partial_y - i\mathcal{A}_2\right)\left(e^{-i\theta}\xi\right) + me^{-i\theta}\xi, \\
\psi &= e^{-i\theta}\left[\gamma_1\left(\partial_x - i\{\mathcal{A}_1 + \theta_x\}\right) + \gamma_2\left(\partial_y - i\{\mathcal{A}_2 + \theta_y\}\right) + mI\right]\xi,
\end{aligned} \tag{2.11}$$

where $\theta_x = \partial_x\theta$ and $\theta_y = \partial_y\theta$. Thus,

$$\left[\gamma_1\widetilde{\nabla}_x + \gamma_2\widetilde{\nabla}_y + mI\right]^{-1}e^{i\theta}\psi = \xi,$$

implying

$$\left[\gamma_1\widetilde{\nabla}_x + \gamma_2\widetilde{\nabla}_y + mI\right]^{-1}e^{i\theta}\psi = e^{i\theta}\left[\gamma_1\nabla_x + \gamma_2\nabla_y + mI\right]^{-1}\psi.$$

This shows that if fermion field ψ is transformed according to $\psi \mapsto e^{i\theta(x,y)}\psi$, then the gauge field must transform as $\mathcal{A} \mapsto \mathcal{A} + \nabla\theta$ to obtain covariance.

A simple consequence of these facts is the following: suppose we are given continuum data $\mathcal{A}$ and f. Then we define the related gauge field and source terms $\widetilde{\mathcal{A}} = \mathcal{A} + \nabla\theta$ and $\widetilde{f} = e^{i\theta}f$. It is easy to check, using the principle of gauge covariance, that if ψ is the solution to the continuum Dirac equation with data $\mathcal{A}$ and f, then the solution with the modified data should be $\widetilde{\psi} = e^{i\theta}\psi$. We use this fact as a basis for a test of the gauge covariance of our discrete algorithm.

EXAMPLE 2. Consider the continuum Dirac equation with gauge field $\mathcal{A}$, which we write as

$$\mathcal{D}\left(\mathcal{A}\right)\psi = f. \tag{2.12}$$

Now, suppose we compute a Helmholtz decomposition of the gauge field $\mathcal{A}$ such that

$$\mathcal{A} = \mathcal{A}_0 + \nabla\omega,$$

where $\mathcal{A}_0$ is divergence free and $\omega \in \mathcal{V}_{\tilde{h}}$. Then (2.12) becomes

$$\mathcal{D}\left(\mathcal{A}_0 + \nabla\omega\right)\psi = f, \tag{2.13}$$

to which the solution is

$$\psi = [\mathcal{D}(\mathcal{A}_0 + \nabla\omega)]^{-1} f. \tag{2.14}$$

Rewrite the source function as $f = e^{i\omega} g$ for some $g \in \mathcal{V}_c$. Then (2.14) becomes

$$\psi = [\mathcal{D}(\mathcal{A}_0 + \nabla\omega)]^{-1} e^{i\omega} g. \tag{2.15}$$

But, from gauge covariance of the propagator, we know that

$$\psi = e^{i\omega} [\mathcal{D}(\mathcal{A}_0)]^{-1} g,$$

implying

$$\psi = e^{i\omega} [\mathcal{D}(\mathcal{A}_0)]^{-1} e^{-i\omega} f.$$

Now, suppose that we wish to solve the same problem but with rotated data. In this case the Dirac equation becomes

$$\mathcal{D}(\widetilde{\mathcal{A}})\widetilde{\psi} = \widetilde{f}. \tag{2.16}$$

The Helmholtz decomposition of $\widetilde{\mathcal{A}}$ is

$$\widetilde{\mathcal{A}} = \mathcal{A}_0 + \nabla\omega + \nabla\theta,$$

and the Dirac equation becomes

$$\mathcal{D}(\mathcal{A}_0 + \nabla\omega + \nabla\theta)\widetilde{\psi} = \widetilde{f}. \tag{2.17}$$

Writing the source term as $\widetilde{f} = e^{i(\omega+\theta)}\widetilde{g}$ the solution becomes

$$\widetilde{\psi} = [\mathcal{D}(\mathcal{A}_0 + \nabla\omega + \nabla\theta)]^{-1} e^{i(\omega+\theta)}\widetilde{g}. \tag{2.18}$$

Again, by gauge covariance, the solution becomes

$$\widetilde{\psi} = e^{i(\omega+\theta)} [\mathcal{D}(\mathcal{A}_0)]^{-1} \widetilde{g},$$

implying

$$\begin{aligned}\widetilde{\psi} &= e^{i(\omega+\theta)} [\mathcal{D}(\mathcal{A}_0)]^{-1} e^{-i(\omega+\theta)} \widetilde{f} \\ &= e^{i\theta}\{e^{i\omega} [\mathcal{D}(\mathcal{A}_0)]^{-1} e^{-i\omega} f\}.\end{aligned}$$

Thus, $\widetilde{\psi} = e^{i\theta}\psi$, as desired.

The key to retaining this property in the discrete setting is that the quark propagator, computed in both cases, is constructed with the same gauge field, $\mathcal{A}_0$, and the same source term, $e^{-i\omega}f$. As such, we must be able to efficiently compute a discrete Helmholtz decomposition of the gauge field, A^h. Fortunately, the choice to represent the gauge field by Nedelec elements makes this fairly easy. Given any $A^h \in \mathcal{W}^h$, there exists a unique $q^h \in \mathcal{V}_{\mathbb{R}}^h$ such that

$$A^h = A_0^h + \nabla q^h,$$

where $q^h \in \mathcal{V}_{\mathbb{R}}^h$ is a bilinear function and A_0^h is characterized by the property that

$$\left\langle A_0^h, \nabla v^h \right\rangle = 0 \ \ \forall v^h \in \mathcal{V}_{\mathbb{R}}^h. \tag{2.19}$$

A vector in $\mathcal{V}_{\mathbb{R}}^h$ that satisfies (2.19) is known as a weak curl [8]. The decomposition can be accomplished by solving the least-squares problem

$$q^h = \arg \min_{v^h \in \mathcal{V}_{\mathbb{R}}^h} \|A^h - \nabla v^h\|_0^2, \tag{2.20}$$

which is equivalent to the weak form

$$\left\langle \nabla q^h, \nabla v^h \right\rangle = \left\langle A^h, \nabla v^h \right\rangle \ \ \forall v^h \in \mathcal{V}_{\mathbb{R}}^h.$$

This weak formulation yields a linear system that is equivalent to that involved in the solution of Poisson's equation with periodic boundary conditions using a Galerkin finite-element method. It is easily solved by standard geometric multigrid methods.

Now we write down a new discrete algorithm which is gauge covariant. First, given $\underline{q} \in \mathcal{N}_{\mathbb{R}} \subset \mathcal{N}_{\mathbb{C}}$, defined on the lattice sites, let $\underline{\Omega}_{\underline{q}}$ be the $n^2 \times n^2$ complex-valued matrix with the quantity e^{iq_j} in the jth diagonal position, and 0.0 elsewhere. Notice then, that $\underline{\Omega}_{\underline{q}}^*$ is also diagonal, and has e^{-iq_j} in the jth diagonal position. Both $\underline{\Omega}_{\underline{q}}$ and $\underline{\Omega}_{\underline{q}}^*$ are unitary matrices.

ALGORITHM 2: Gauge Covariant Least-Squares Dirac Solve

- *Input:* Gauge field $\underline{A}$, source term $\underline{f}$.
- *Output:* Wavefunction $\underline{\psi}$.

1. Map $\underline{A} \mapsto A^h \in \mathcal{W}^h$.
2. Compute $A^h = A_0^h + \nabla q^h$.
3. Map $q^h \to \underline{q}$.
4. Set $\underline{g}_u = \underline{\Omega}_{\underline{q}}^* \, \underline{f}_u$ and $\underline{g}_d = \underline{\Omega}_{\underline{q}}^* \, \underline{f}_d$.
5. Map $\underline{g} \mapsto g^h \in \left(\mathcal{V}_{\mathbb{C}}^h\right)^2$.
6. Find $\phi^h \in \left(\mathcal{V}_{\mathbb{C}}^h\right)^2$ s.t. $\left\langle \mathcal{D}\phi^h, \mathcal{D}v^h \right\rangle = \left\langle g^h, \mathcal{D}v^h \right\rangle \quad \forall v^h \in \left(\mathcal{V}_{\mathbb{C}}^h\right)^2$, where $\mathcal{A} = A_0^h$.
7. Map $\phi^h \mapsto \underline{\phi} \in \mathcal{N}_{\mathbb{C}}^2$.
8. Set $\underline{\psi}_u = \underline{\Omega}_{\underline{q}} \, \underline{\phi}_u$ and $\underline{\psi}_d = \underline{\Omega}_{\underline{q}} \, \underline{\phi}_d$.

Note also that Steps 5-7 can replaced by the familiar matrix operation

$$\underline{\phi} = \mathbb{A}^{-1}\mathbb{G}\underline{g}, \tag{2.21}$$

where matrices $\mathbb{A}$ and $\mathbb{G}$ were constructed using the grad-free gauge field, A_0^h.

There is significant motivation for formulating the discrete algorithm in a gauge covariant way, despite the minor increase in computational cost, due to the Helmholtz decomposition. In the Monte Carlo process it is desirable to generate gauge fields that are statistically distinct from one another. If one gauge field can be generated from another through the application of local gauge transformations, then we say the two configurations are in the same equivalence class. Formally, given $\underline{q} \in \mathcal{N}_{\mathbb{R}}$, define $[\Delta_x \underline{q}, \Delta_y \underline{q}]^T \in \mathcal{E}$ such that

$$\left[\Delta_x \underline{q}\right]_{(k+1/2,l)} = \frac{q_{(k+1,l)} - q_{(k,l)}}{h}, \tag{2.22}$$

where $q_{(k,l)}$ is the value of $\underline{q}$ associated with the k^{th} lattice site in the x-direction and the l^{th} lattice site in the y-direction. The subscript $(k+1/2, l)$ indicates that the value is associated with the lattice link between the lattice sites (k, l) and $(k+1, l)$. Similarly, define

$$\left[\Delta_y \underline{q}\right]_{(k,l+1/2)} = \frac{q_{(k,l+1)} - q_{(k,l)}}{h}. \tag{2.23}$$

DEFINITION 1: We say the pairs $(\underline{\psi}, \underline{A})$ and $(\widetilde{\underline{\psi}}, \widetilde{\underline{A}})$ are in the same equivalence class if there exist $\underline{q} \in \mathcal{N}_{\mathbb{R}}$ such that

$$\widetilde{\underline{\psi}} = \left[\widetilde{\underline{\psi}}_u,\ \widetilde{\underline{\psi}}_d\right]^t = \left[\underline{\Omega_q}\underline{\psi}_u,\ \underline{\Omega_q}\underline{\psi}_d\right]^t,$$

and

$$\widetilde{\underline{A}} = \left[\widetilde{\underline{A}}_1,\ \widetilde{\underline{A}}_2\right]^t = \left[\underline{A}_1 + \Delta_x \underline{q},\ \ \underline{A}_2 + \Delta_y \underline{q}\right]^t.$$

THEOREM 1: Suppose $(\underline{f}, \underline{A})$ and $(\widetilde{\underline{f}}, \widetilde{\underline{A}})$ are in the same equivalence class. Then, Algorithm 2 yields $\underline{\psi}$ and $\widetilde{\underline{\psi}}$ such that

$$\underline{\psi} = [\underline{\psi}_u, \underline{\psi}_d]^t = \left[\underline{\Omega_q}\ \widetilde{\underline{\psi}}_u,\ \underline{\Omega_q}\ \widetilde{\underline{\psi}}_d\right]^t.$$

PROOF: The proof follows directly from Definition 1 and the development of Algorithm 2. □

2.3. Chiral Symmetry. In the broadest sense, chiral symmetry is a global symmetry property that, in the massless case, independent transformations of the spin-up and spin-down fields do not change the physics of the model. This property is manifested mathematically by setting $m = 0$, and assuming that ψ is the solution of the continuous Dirac equation with source term f. That is, assume

$$\mathcal{D}_0\psi = f,$$

where $\mathcal{D}_0$ is the massless Dirac operator in the continuum. Next, define a global transformation Ω, such that

$$\Omega = \begin{bmatrix} e^{i\theta_u} & 0 \\ 0 & e^{i\theta_d} \end{bmatrix}.$$

Then, define rotated wavefunction, $\widetilde{\psi} = \Omega\psi$, and rotated source term, $\widetilde{f} = \Omega f$. We say that our theory has chiral symmetry if

$$\mathcal{D}_0\widetilde{\psi} = \widetilde{f}. \tag{2.24}$$

It is important to note the difference between the requirements of chiral symmetry and those of gauge covariance. First, we are not permitted to alter $\mathcal{D}_0$ to make (2.24) hold. Second, chiral symmetry is a *global* symmetry, which is why θ_u and θ_d, in the definition of Ω, do not have spatial dependence. All spin-up and spin-down fields are rotated by the same transformation at each point.

In the discrete setting, we recall that solving the Dirac equation amounts to solving the matrix equation

$$\mathbb{A}\underline{\psi} = \mathbb{G}\underline{f}. \tag{2.25}$$

where, in the massless case,

$$\mathbb{A} = \begin{bmatrix} \mathbb{A}_{11} & 0 \\ 0 & \mathbb{A}_{22} \end{bmatrix}, \quad \mathbb{G} = \begin{bmatrix} 0 & \mathbb{B}_x - i\mathbb{B}_y \\ \mathbb{B}_x + i\mathbb{B}_y & 0 \end{bmatrix}.$$

Given phase factors $\theta_u, \theta_d \in \mathbb{R}$, define the discrete global transformation $\underline{\Omega} \in \mathbb{C}^{2n^2 \times 2n^2}$ by

$$\underline{\Omega} = \begin{bmatrix} e^{i\theta_u} I & 0 \\ 0 & e^{i\theta_d} I \end{bmatrix}.$$

Where I is the $n^2 \times n^2$ identity matrix. We say that our discrete formulation has chiral symmetry if, given $\underline{\psi}$ and $\underline{f}$ satisfying (2.25), rotated vectors $\underline{\widetilde{\psi}} = \underline{\Omega\psi}$ and $\underline{\widetilde{f}} = \underline{\Omega f}$ also satisfy (2.25). Clearly, this is true in the least-squares formulation. To see this,

$$\begin{aligned} \mathbb{A}\underline{\psi} &= \mathbb{G}\underline{f}, \\ \mathbb{A}\underline{\Omega}^*\underline{\Omega}\ \underline{\psi} &= \mathbb{G}\underline{\Omega}^*\underline{\Omega}\ \underline{f}, \\ \underline{\Omega}^*\mathbb{A}\underline{\Omega}\ \underline{\psi} &= \underline{\Omega}^*\mathbb{G}\underline{\Omega}\ \underline{f}, \end{aligned}$$

since, because of their block forms in the massless case, $\mathbb{A}$ and $\mathbb{G}$ commute with $\underline{\Omega}^*$. This implies,

$$\mathbb{A}\underline{\Omega}\,\underline{\psi} = \mathbb{G}\underline{\Omega}\,\underline{f},$$
$$\mathbb{A}\underline{\tilde{\psi}} = \mathbb{G}\underline{\tilde{f}},$$

as desired.

2.4. Species Doubling. A concern in the numerical analysis of the field equations for QCD is the problem of *species doubling*. We illustrate this phenomenon by returning to the 1D Schwinger model. In CoFD formulations, the massless discrete Dirac operator in the absence of a gauge field is given by

$$\mathbb{D} = \gamma_1 \nabla_1^h. \tag{2.26}$$

The so-called *naive* discretization corresponds to the discretization of covariant derivative ∇_1 using central differences:

$$\nabla_1^h = \frac{\psi(x+h) - \psi(x-h)}{2h}. \tag{2.27}$$

Transforming D into Fourier space, we obtain the dispersion relation

$$R(p) = -i\frac{\gamma_1 \sin(ph)}{h} \tag{2.28}$$

or, in full matrix notation,

$$R(p) = -i\begin{bmatrix} 0 & \frac{\sin(ph)}{h} \\ \frac{\sin(ph)}{h} & 0 \end{bmatrix}.$$

The eigenvalues of dispersion relation R are associated with the energy of the system and are given by

$$E = \sqrt{\frac{1}{h^2}\sin^2(ph)}.$$

For the results to be physical, as the lattice spacing $h \to 0$, we require that the energy in the system not diverge. In the above expression, this happens when $p = 0$ or $\pm\pi/h$. Note that these frequencies correspond to zeros of the dispersion relation, $R(p)$. Also, notice that we do not consider $p = \pm n\pi/h$ for $n > 1$ because modes of these frequencies cannot be represented on the lattice. The range of possible frequencies, $-\pi/h \leq p \leq \pi/h$, is called the Brillouin zone. The problem arises because the three physical frequencies $p = 0, \pm\pi/h$ correspond to multiple particles described by the same theory, which is not physical. By periodicity, the particles described by $p = \pi/h$ and $p = -\pi/h$ are the same so this formulation represents two distinct particles when there should only be one. Hence, the phenomenon is called species doubling [6].

The usual fix is to add an artificial stabilization term to D. This is the basis for the Dirac-Wilson operator, which is given in 1D by

$$\mathbb{D} = \gamma_1 \nabla_1^h + \frac{\kappa h}{2} \gamma_0 \Delta^h. \tag{2.29}$$

In the free case, the dispersion relation for the Dirac-Wilson operator looks like

$$R(p) = -i\frac{\gamma_1 \sin(ph)}{h} + \frac{\kappa I\left[1 - \cos(ph)\right]}{h}. \tag{2.30}$$

In this case, $p = 0$ is still a root of the dispersion relation, but now

$$R(\pm\pi/h) = \frac{2\kappa}{h},$$

so the Dirac-Wilson operator does not suffer from species doubling. This comes at a high price however, to avoid species doubling it was necessary to add a nonphysical term to the operator. Furthermore, the additional term appears on the main diagonal of $\mathbb{D}$, thus breaking chiral symmetry.

To see if this is a problem for the least-squares discretization, consider (??), the general form of the least-squares version of $\mathbb{D}$. Since we ignore the gauge field, terms $P^*\mathcal{B}^*\mathcal{B}P$ and $P^*\mathcal{B}\mathcal{B}^*P$ are just the usual finite element discretization of the standard Laplacian. Similarly, terms $P^*\mathcal{B}P$ and $P^*\mathcal{B}^*P$ are the usual Galerkin discretization of the first derivative operator. Thus, $\mathbb{D}$ in one dimension becomes

$$\mathbb{D} = \gamma_1 \left[\frac{\psi(x+h) - \psi(x-h)}{2h}\right]^{-1} \left[\frac{\psi(x+h) - 2\psi(x) + \psi(x-h)}{h^2}\right]$$

The corresponding dispersion relation is given by

$$R(p) = \frac{\left[1 - \cos(hp)\right]/h}{i\,\sin(hp)}.$$

Clearly, $p = 0$ is the only root of R. In fact, $R \to \infty$ as $p \to \pm\pi/h$. Thus, the least-squares formulation does not suffer from species doubling.

3. Numerical Experiments. In this section, we explore the use of a multilevel iterative method for solving the matrix system (2.21), that takes the place of Steps 5-7 of Algorithm 2. To avoid working in complex arithmetic, we solve the equivalent real formulation of Eq. (2.21):

$$\begin{bmatrix} \mathbb{X} & -\mathbb{Y} \\ \mathbb{Y} & \mathbb{X} \end{bmatrix} \begin{bmatrix} \underline{x} \\ \underline{y} \end{bmatrix} = \begin{bmatrix} \underline{a} \\ \underline{b} \end{bmatrix}, \tag{3.1}$$

where $\mathbb{X}, \mathbb{Y}$ are real-valued matrices satisfying $\mathbb{A} = \mathbb{X} + i\mathbb{Y}$, $\underline{\phi} = \underline{x} + i\underline{y}$, and $\mathbb{G}\underline{g} = \underline{a} + i\underline{b}$.

3.1. Smoothed Aggregation Multigrid. We wish to use a multilevel method to solve (3.1). Multigrid methods are a class of iterative algorithms used to solve linear systems of the form $Au = f$ that can be shown to be optimal in the sense of accuracy gained per computational cost. Multigrid methods rely on two complementary processes to reduce the error in each successive iterate. Relaxation is a *local* process that reduces a large portion of the error in a relatively inexpensive way. Error that relaxation fails to adequately reduce is called *algebraically smooth*. Coarse-grid correction is a *global* process that is designed to complement relaxation by reducing the algebraically smooth error. This process works by doing relaxation on a fine grid until only smooth error remains, and then moving to a coarser-grid and solving for a lower dimensional representation of the error. The coarse grid approximation to the error is then taken back up to the fine grid through an interpolation process and used to correct the approximate there. The success of the coarse-grid correction process depends on how accurately smooth error modes can be represented on the coarse grid.

For many problems in the physical sciences, the algebraically smooth error modes are geometrically smooth as well. Standard geometric multigrid methods are usually very effective at solving these problems. Unfortunately, due to the random nature of the background gauge fields in QCD, the smooth error modes are in no way geometrically smooth. In Figure 3.1, we see that both the real and imaginary components of the smooth error are highly oscillatory. These plots were obtained by applying 100 iterations of Gauss-Seidel on the problem $\mathbb{A}\underline{\phi} = 0$ with a random initial guess.

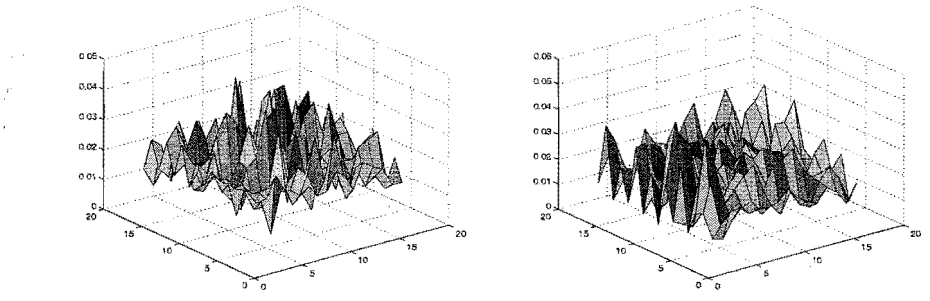

Fig. 3.1: Real and complex components of algebraically smooth error of $\mathbb{A}$ for $m = 0.1$, $\beta = 2$, and $N = 16$. Error was computed using 100 iterations of Gauss-Seidel on $\mathbb{A}\underline{\phi} = 0$ with a random initial guess

Smoothed aggregation multigrid (SA [3]) is a multilevel solver that is based on algebraic smoothness as an abstraction of the property of geometric smoothness used in conventional multilevel algorithms. Given prototype representations of algebraically smooth error, SA automatically builds intergrid transfer operators that attempt to represent all smooth error modes on coarser grids, regardless of their geometric smoothness. Unfortunately, this requires *a priori* knowledge of the prototype modes. Randomness of the background fields in QCD applications causes the nature of the smooth error to vary widely between different gauge configurations and, in any case, little is known about their local character. We turn instead to adaptive smoothed aggregation multigrid (αSA [4]), which uses a setup procedure to first expose these problematic error components, and then builds a multigrid process to effectively reduce them.

3.2. Results. Table 3.1 reports convergence factors of conjugate gradients (CG) preconditioned by αSA applied to the homogeneous version of (3.1) for various values of the particle mass, m, and gauge field temperature β. The αSA preconditioner was based on V(2,2)-cycles and 3 grid levels. The aggregation process was performed algebraically and the relaxation scheme was nodal Gauss-Seidel. Finally, 8 prototype error components were found during the adaptive setup process and used to define the intergrid transfer operators in the V-cycle. A single V(2,2)-cycle was used as the preconditioner in the CG solve. For comparison, convergence factors for diagonally preconditioned CG are also provided in Table 3.1.

β/m	.01	.1	.3
2	.21 / .98	.20 / .94	.20 / .94
3	.25 / .98	.24 / .95	.22 / .94
5	.23 / .97	.23 / .94	.21 / .93

β/m	.01	.1	.3
2	.32 / .98	.31 / .96	.32 / .94
3	.36 / .99	.34 / .95	.34 / .95
5	.32 / .96	.38 / .94	.41 / .92

Table 3.1: Average convergence factors for αSA preconditioned CG and diagonally preconditioned CG applied to (2.21) on 64×64 (top) and 128×128 (bottom) lattices with varying choices of mass parameter m and temperature β.

Notice that, as mass parameter m is decreased, the performance of the solver remains fairly static. This is an important result because it means that the problem of critical slowing down has been greatly reduced.

In addition to good convergence rates, our formulation generally improves computational cost per multigrid cycle over conventional solvers applied to (2.1) by avoiding the added complexity of these discrete normal equations. Our least-squares approach does form normal equations, but more effectively on the continuum Dirac operator only, without the additional stabilization term. Discretizing the continuum normal equations in this way results in a stencil that has only the nearest-neighbor connections typical of a second-order operator, in contrast to the wider and more complicated stencils for the normal equations of the Dirac-Wilson matrix. As a result, the least-squares matrix is more compact and has about 30% fewer nonzeros than the Dirac-Wilson matrix.

Also, the *operator complexity* in the multigrid cycle based on the least-squares formulation is significantly better than those observed in formulations based on CoFDs [1]. The operator complexity is defined as the ratio of the total number of degrees of freedom on all grids in the multigrid hierarchy to the number of degrees of freedom on the finest grid. This number indicates how much work has to be done on the coarse grids compared to that on the fine grid. For the lattice sizes that were tested in these experiments operator complexity stayed bounded below 1.5, a very satisfactory result.

4. Conclusions. We described a discretization of the continuous Dirac equation for the 2D Schwinger model of QED based on least-squares finite elements. The formulation avoids several pitfalls of traditional discretizations based on covariant finite differences by producing a discrete operator that is Hermitian, positive definite, and

extremely sparse. We argued that it retains a sense of global chiral symmetry and avoids the need for irrelevant stabilization terms by not suffering from species doubling. Furthermore, we show that the resulting discrete system can be handled quite effectively by conjugate gradient with adaptive smoothed aggregation as a preconditioner.

Acknowledgments. The authors wish to thank Achi Brandt of the Weizmann Institute, Rich Brower, Claudio Rebbi, and Mike Clark of Boston University, and Pavlos Vranas of Lawrence Livermore National Lab, for their many useful comments and clarifications.

REFERENCES

[1] J. Brannick, M. Brezina, D. Keyes, O. Livne, I. Livshits, S. MacLachlan, T. Manteuffel, S. McCormick, J. Ruge, and L. Zikatanov, Adaptive Smoothed Aggregation in Lattice QCD, Lecture Notes Comp. Sci. Eng., 55 (2006), pp. 499-506.

[2] J. Brannick, R.C. Brower, M.A. Clark, J.C. Osborn, C. Rebbi, Adaptive Multigrid Algorithm for Lattice QCD, Phys. Lett., 100 (2008).

[3] P. Vanek, J. Mandel, and M. Brezina, Algebraic Multigrid by Smooth Aggregation for Second and Fourth Order Elliptic Problems, Computing, 56 (1996), pp. 179-196.

[4] M. Brezina, R. Falgout, S. MacLachlan, T. Manteuffel, S. McCormick, and J. Ruge, Adaptive Smoothed Aggregation (αSA), SIAM J. Sci. Comp., 25 (2004), pp. 1896-192.

[5] M. Creutz, Quarks, Gluons and Lattices, Cambridge Univ. Press, Cambridge, 1983.

[6] T. DeGrand, C. DeTar, Lattice Methods for Quantum Chromodynamics, World Scientific, New Jersey, 2006.

[7] W. Griener, S. Schramm, E. Stein, Quantum Chromodynamics, Springer-Verlag, Berlin Heidelberg, 2007

[8] J. C. Nedelec A New Family of Mixed Finite Elements in $\mathbb{R}^3$, Numerische Mathematik, 50 (1986), pp. 57-81

[9] K. Wilson, Confinement of Quarks, Phys. Rev. D, 10 (1974).